Wetlands Ecol Manage
https://doi.org/10.1007/s11273-020-09735-y

ORIGINAL PAPER

Vegetation biomass and carbon stocks in the Parnaíba River Delta, NE Brazil

Mirya Grazielle Torres Portela · Giovana Mira de Espindola · Gustavo Souza Valladares · João Victor Alves Amorim · Jéssica Cristina Oliveira Frota

Received: 10 December 2019 / Accepted: 4 June 2020

Abstract Coastal ecosystems are considered environments with great potential for carbon storage. Given the difficulties in quantifying biomass, allometric equations and remote sensing have become fundamental tools in the studies of quantification of vegetation biomass and carbon stocks. Thus, the objective of this study is to quantify and estimate the spatial distribution of vegetation biomass and to quantify the carbon stock of the Parnaíba River Delta vegetation. The study was carried out in part of the *Parnaíba River Delta Environmental Protection Area* and in the *Parnaíba River Delta Marine Extractive Reserve*, in NE Brazil, in five spots within distinct vegetation types: psammophile pioneer vegetation, dune subevergreen vegetation, mangrove evergreen vegetation, floodplain vegetation and vegetation associated with carnaubals. At 26 collection points, 10 × 20 m plots were marked, in which the diameter at breast height and height of all individuals were measured. The collected data were used in allometric equations for vegetation biomass estimates and these values were converted into carbon stocks. The spatial distribution of aboveground vegetation biomass (AGB) was also estimated by remote sensing, where we extracted and selected spectral variables obtained from Landsat-8 OLI sensor images, on three different dates. Prediction models were calculated by multiple linear regression analysis. It was observed that the mangrove evergreen vegetation obtained higher vegetation biomass and carbon stock than the others. The models obtained through remote sensing that provided the best estimates of AGB were those of November 12th, 2016 (EAM = 6.84; RMSE = 47.89 Mg ha^{-1}; $R^2 = 0.72$) and November 28th, 2016 (EAM = 9.63; RMSE = 34.67 Mg ha^{-1}; $R^2 = 0.58$).

Keywords Coastal ecosystems · Mangrove · Blue carbon · Carbon sequestration · Remote sensing

Introduction

Natural ecosystems are fundamental components of the terrestrial system that must be understood to model and manage atmospheric concentrations of greenhouse gases and thus the global climate (Neubauer and Megonigal 2019). There is a realization that climate change will continue to have fundamental impacts on the natural environment and its relationships (Frank et al. 2015).

According to the IPCC (2014), by the end of the century the planet will have heated between 0.3 and 4.8 °C, and the increase in atmospheric greenhouse gases concentrations leads to gradual average global warming and may change the frequency, the gravity

M. G. T. Portela · G. M. de Espindola (✉) · G. S. Valladares · J. V. A. Amorim · J. C. O. Frota
Department of Geography, Federal University of Piauí (UFPI), Teresina, Brazil
e-mail: giovanamira@ufpi.edu.br

Published online: 10 June 2020

and even the nature of extreme events such as droughts, floods and biological diversity loss.

Forest environments are considered highly productive ecosystems and large storages of carbon from biomass, where estimating and monitoring them has become increasingly important because of their relevance to climate change adaptation and mitigation programs, as well as the importance of forest carbon stocks in the global cycle and global environmental change studies (Frank et al. 2015; Fatoyinbo et al. 2018).

With reference to coastal environments, these are considered to be major contributors to carbon sequestration when compared to other native environments (Alongi 2014). In this sense, we highlight the mangrove environments, which are forest wetlands of ecological and economic importance, with large carbon storage that acts as an important coastal buffer and their protection and restoration has been proposed as an effective mitigation strategy for the climate changes (Fatoyinbo et al. 2018). The carbon stored in these environments is known as "blue carbon" (Cusack et al. 2018).

Although these ecosystems are important for carbon storage, the quantification of carbon in vegetation biomass in these environments has been hampered by the lack of large-scale forest data, especially in peripheral and neglected regions, along the northeast (NE) coast of Brazil.

The Parnaíba River Delta (PRD) is the largest in the open sea of the Americas and one of the few examples of river delta that is still developing under natural conditions, unlike some widely impacted deltas around the world, having importance in wildlife conservation, flora and fishing resources (Silva et al. 2019; de Paula Filho et al. 2015).

Most of the natural environments bring difficulties in relation to fieldwork and forest data collection due to accessibility and cost issues, making it a constant challenge for those working with vegetation biomass (Tang et al. 2016). Given this scenario, strategies to facilitate the quantification of vegetation biomass in species have been developed in order to avoid these barriers. The use of allometric equations for the quantification of vegetation biomass is one of the widely used tools to acquire data quickly and accurately without the need to remove vegetation from the site for biomass quantification in the laboratory.

Another noteworthy approach is the use of remote sensing data. Remote sensing modeling is a crucial option for vegetation biomass estimation, and selecting the best method will have a direct influence on the final results (Lu et al. 2005), something that has been widely evaluated and discussed in several researches in coastal ecosystems (Duncan et al. 2018; Fatoyinbo et al. 2018; Kauffman et al. 2018; Zhang et al. 2018).

Given the above, the study aims to quantify and estimate the spatial distribution of vegetation biomass and quantify the carbon stock of vegetation in the Parnaiba River Delta, located in the semiarid coastal region of NE Brazil. We analyzed a combination of allometric equations and remote sensing data approach to answer the following questions: (i) how does the biomass is spatially distributed within the study area? (ii) how does different selected variables influence this spatial distribution? (iii) how is mangrove biomass spatially distributed and how is its relevance for this ecosystem? Thus, this article shows a first approach to the estimation of vegetation biomass and carbon stocks in a semiarid coastal region in NE Brazil, dominated by mangroves and threatened by anthropogenic pressure.

Material and methods

Characterization of the study area

The study area is located in the Brazilian state of Piauí, NE Brazil, and comprises part of the *Parnaíba River Delta Environmental Protection Area* (APA—acronyms in Portuguese) and part of the *Parnaíba River Delta Marine Extractive Reserve* (Resex—acronyms in Portuguese), more precisely, in the region bounded by the Igaraçu River to the southeast, Parnaíba River to the west, and the Atlantic Ocean to the north, encompassing the municipality of Ilha Grande, and part of the municipality of Parnaíba (Fig. 1). The area of study has approximately 282 km^2, of which 8 km^2 belong to the Resex.

The study area is under the regulation of Brazilian Federal Law N° 9,985 of July 18th, 2000, which establishes the Brazilian National System of Nature Conservation Units (SNUC—acronyms in Portuguese) (Brazil 2000a). This law divides conservation units into integral protection units and sustainable use

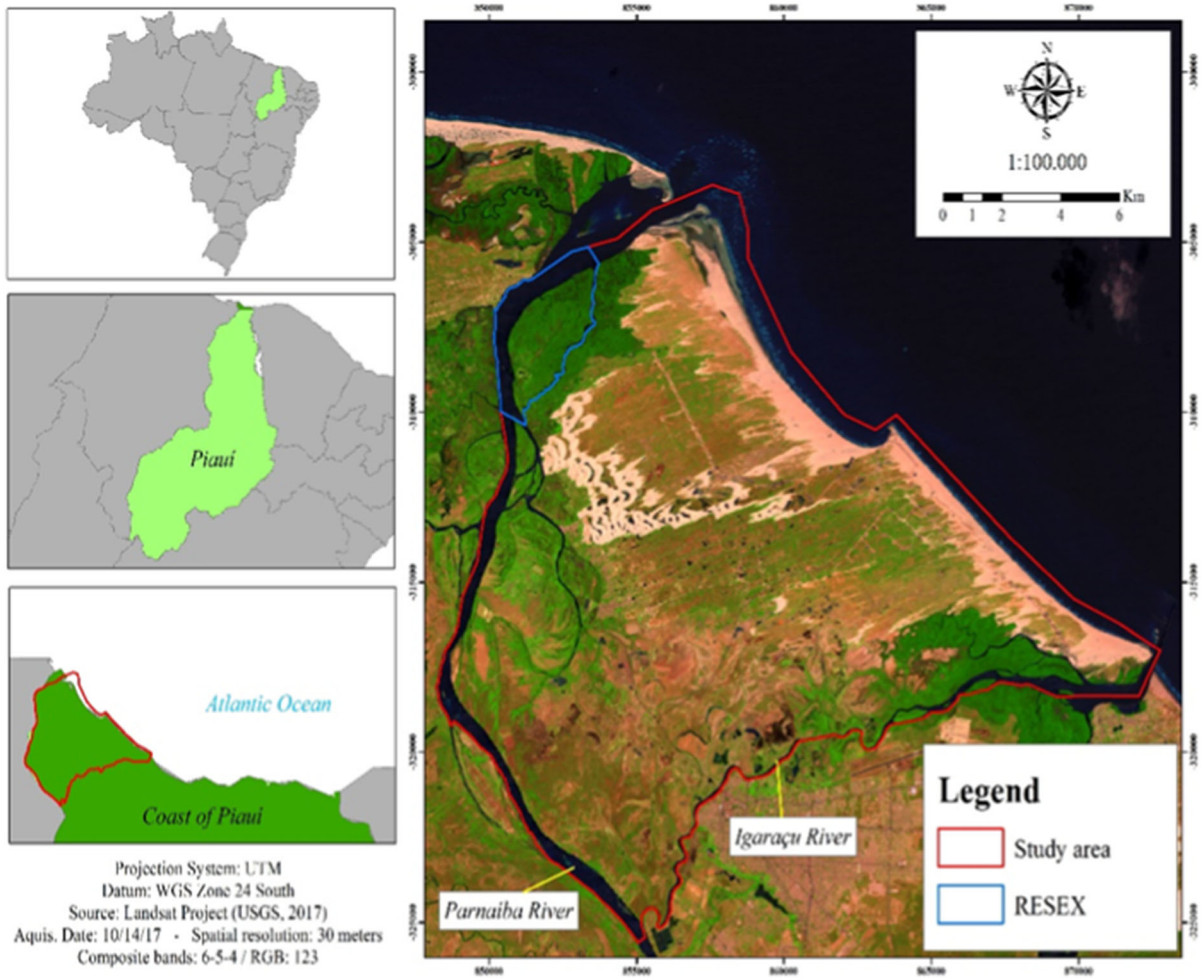

Fig. 1 Location of the study area

units. The two conservation units present in the study area are categorized as sustainable use units.

The APA was created by the Federal Government by Decree of August 28th, 1996, aiming to protect the Parnaíba, Timonha and Ubatuba Rivers, occupying an approximate area of 3,138 km^2 (Brazil 1996). It presents a mosaic of ecosystems interspersed by bays and estuaries in a very dynamic marine fluvial region, formed by the ecological tension between Cerrado and Caatinga biomes and marine systems (Guzzi 2012).

The Resex was created by Decree of November 16th, 2000, with an area of approximately 270 km^2, with the objective of guaranteeing the self-sustainable exploitation and conservation of renewable natural resources traditionally used by the area's extractive population (Brazil 2000b).

The coastal plain of Piauí has high levels of rainfall, however, with values that vary greatly throughout the year, with maximum monthly precipitation approaching 300 mm (Sousa et al. 2016). As for pedology, in general, the main orders of soils found in the study area were the Neosols (Quartzhenic and Fluvic), Planosols, Gleysols, Spodosols, Cambisols and Vertisols (Cabral 2018).

The study region presented in the year of 2016 precipitation that extended until July and months with no accumulated precipitation, with average monthly temperature reaching 35 °C in September (Fig. 2). Comparing with the climatological normal of precipitation in 30 years, rainfall in this period was lower than expected, although the northeast of Brazil was affected by severe drought between the years of 2012

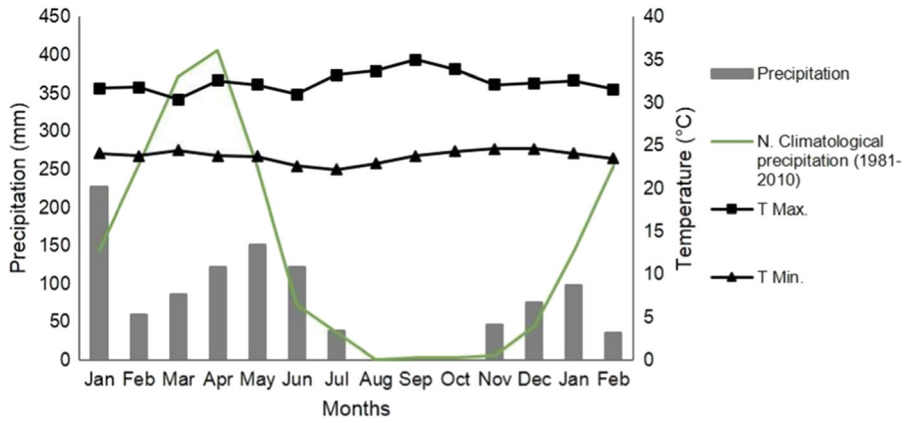

Fig. 2 Precipitation data (mm) and maximum and minimum temperature (°C) of the study area from January 2016 to February 2017 and climatological normal rainfall from 1981 to 2010. *Source* INMET (2018)

and 2015, causing impacts not seen in previous decades (Marengo et al. 2017), which may have had an influence on vegetation.

As it is a sustainable use conservation unit, classified by the SNUC, the study area has part of its area occupied by housing, agricultural activities and wind energy production, with restricted access areas. The study region has a vegetal biodiversity translated into the various types of vegetation found, which predominate in the landscape and mix with other formations such as coastal trays, Cerrado and Caatinga vegetation.

According to Costa and Cavalcanti (2010), the vegetation present in the area has the majority of its woody species, characterized by spaced trees with irregular crowns and a secondary aspect, interposed by subsistence agriculture. Moreover, it also has the presence of secondary physiognomy vegetation with significant interpenetration of typical Caatinga species, unique in the world, which makes it an important differential in the quantification of vegetation biomass in this environment, when compared to other deltaic regions of the world.

Our study was conducted from December 2016 to February 2017, in five areas with distinct vegetation within the study area, classified according to Fernandes et al. (1996): psammophile pioneer vegetation, dune subevergreen vegetation, mangrove evergreen vegetation, floodplain vegetation and vegetation associated with carnaubals (Fig. 3).

Determination of sampling points

The points to conduct the field data survey were previously defined, considering areas of great representation regarding the vegetation structure. The accessibility characteristics of the APA were taken into consideration due to the presence of privately-owned areas, forests, dunes and other difficult-to-traffic lands. In this sense, collection points with better accessibility for the work team were chosen, but taking the precaution of keeping at least 100 m from the edges or roads and looking for the closest possible points to those previously defined. Thus, for the field vegetation data collection, 26 points were determined, distributed to the five vegetation types (Fig. 4).

Quantification of vegetation biomass

For the analysis of the vegetation biomass of the study area, we made a forest inventory, launching 26 rectangular sampling units of 200 m^2 (10 $\times$ 20 m), based on the one proposed by Fundación Solar (2010), Kauffman and Donato (2012) and Lima Junior et al. (2014). The authors suggest sampling units in circular models, square and rectangular up to 1000 m^2 in area. We considered and used the rectangular model in all units, as it is the most interesting model for the studied region, which presented difficulties of access and dense vegetation and, in some places, interlaced.

Although larger models harbor a larger number of plant individuals, this sampling model is also capable

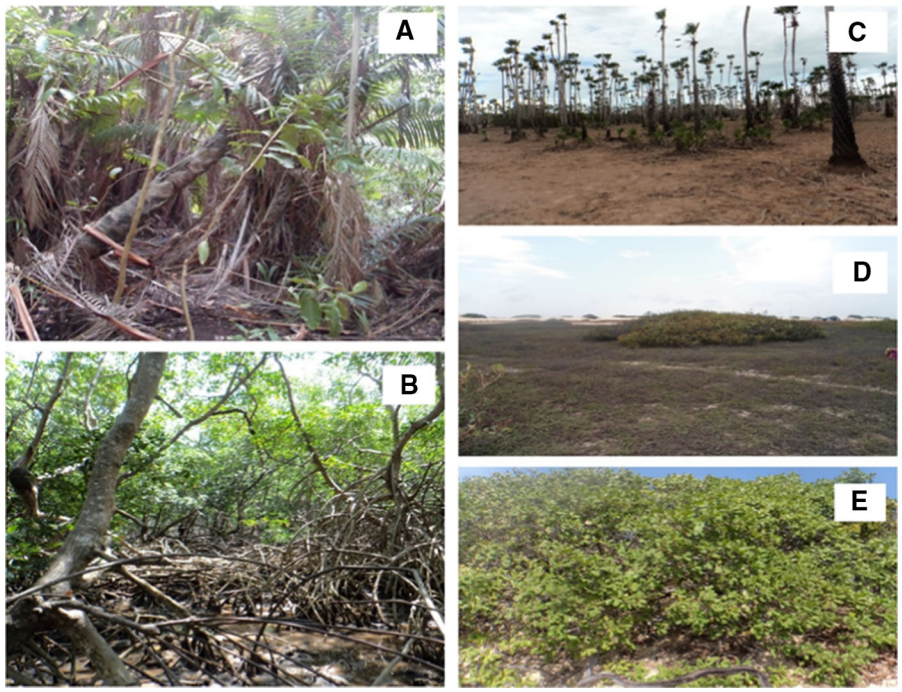

Fig. 3 Vegetation types evaluated in the study. Floodplain vegetation (**a**); mangrove evergreen vegetation (**b**); vegetation associated with carnaubals (**c**) psammophile pionner vegetation (**d**); and dune subevergreen vegetation (**e**)

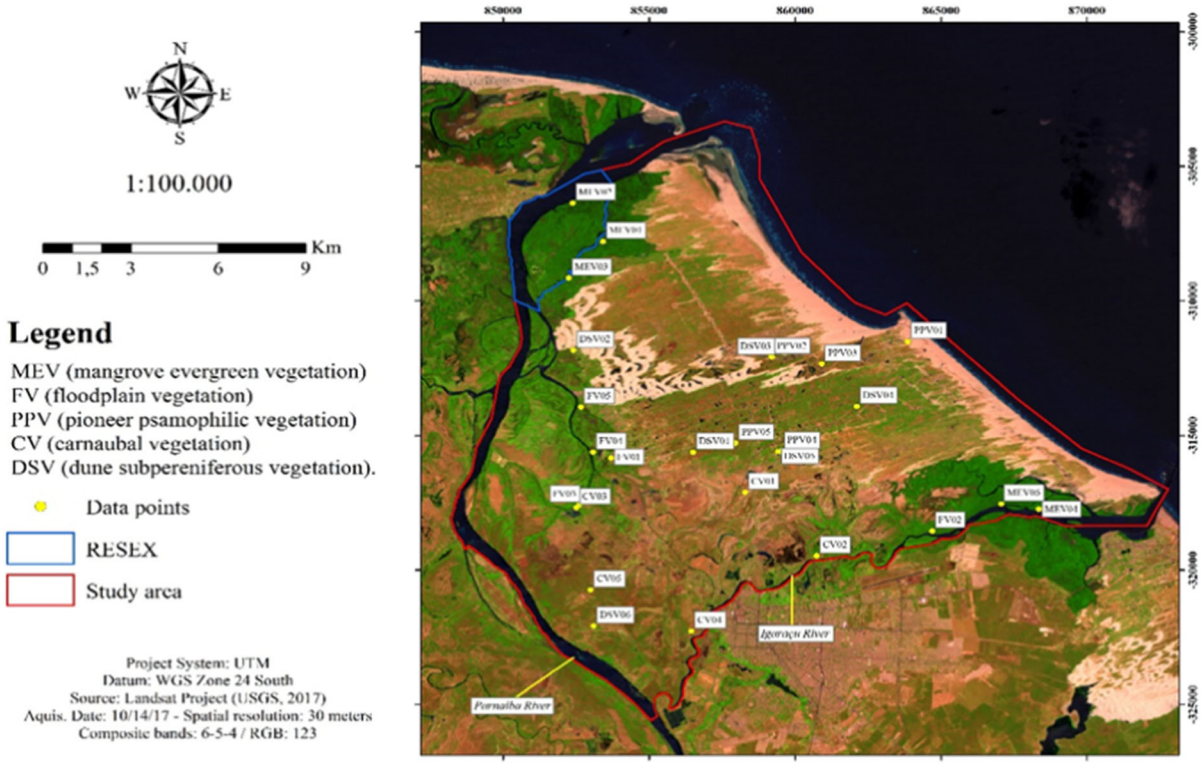

Fig. 4 Localization of data points determined in study area, according with five vegetation types

of satisfactorily representing plant strata, larger models, highlighting the need to verify the measurement of all individuals within the sample unit and seek to move away from the banks of rivers, roads and homes. The vegetation biomass estimate was subdivided into three fractions: hypogeal, epigeal and litter biomass.

For the dune subevergreen vegetation, floodplain vegetation and vegetation associated with carnaubals, we use the one proposed by Lima Júnior et al. (2014) and Fundación Solar (2010). To determine the biomass of the first fraction of the vegetation, within each plot, we measured the plants with diameter at breast height (DBH) greater than 3 cm (CAP 9.42–94.25 cm) and height, disregarding plants with DBH below 3 cm and considering standing and fallen dead individuals. To measure vegetation biomass for mangrove, the methodology proposed by Kauffman and Donato (2012) was followed considering DBH measures, including those of standing and fallen dead individuals, in addition to height.

After data collection and tabulation, we calculated the biomass of live and dead trees by allometric equations, appropriate for each species or for a specific vegetation. For typical species from the Caatinga, the Brazilian dry forest, we used equations of Lima Júnior et al. (2014), for palmaceous we used the equation of Frangi and Lugo (1985), for red mangrove (*Rhizophora mangle*) we used the equation of Santos et al. (2017), and for white mangrove (*Laguncularia racemosa*) and black mangrove (*Avicennia germinans*) we used the equation of Fromard et al. (1998).

The biomass of standing dead mangrove trees was determined as suggested by Kauffman et al. (2012), by calculating the equations used for living trees and reducing the values from 10 to 20% depending on the individual's decay.

For dead standing trees of other species, an equation proposed by Brown et al. (1989) was used for live trees, provided that there is a 30% discount on biomass. For fallen logs the formula proposed by Fundación Solar (2010), based on DBH and height values, was used to calculate basal area and wood density. The values for wood density of the species were searched in the literature (Maia 2004). For species for which these values for wood density were not found, a value of 0.5 was used, according to Fundación Solar (2010).

The biomass of litter and psammophile pioneer vegetation was determined by the direct method. In each plot, a circumference of 0.3 m^2 was randomly thrown three times, collecting all the material contained within it. After the removal of the material, it was weighed at the time of collection or cutting (in the case of pioneer psamophilous vegetation), dried in an oven at 65 °C until constant temperature and the material was then dried.

To determine below ground biomass in mangrove plants, the equation proposed by Komiyama et al. (2005) was used. For the other species, the determination of below ground biomass was calculated considering a percentage of 30% of the above ground biomass calculated for these species, following what was proposed by MacDicken (1997). After obtaining the vegetation biomass data, the values were converted to biomass carbon using an IPCC (2007) conversion factor of 0.5. Biomass and carbon data were statistically analyzed by the Tukey test at 5% probability.

Spatial distribution of vegetation biomass by remote sensing

To estimate above ground biomass (AGB), the methodology proposed by Lu et al. (2005) and Lima Junior (2014) was used, with adaptations, consisting of very detailed steps. The first step consisted in the selection of data samples collected in the field, used as reference data for model validation (Naessens et al. 2012). In the study 35 training points and 8 prediction validation points were used, making a total of 43 points, following the sample pattern of studies conducted with remote sensing biomass quantification reviewed by Fassnacht et al. (2014).

The second stage consisted of the extraction and selection of remote sensing variables. Spectral variables were obtained from Landsat-8 OLI (Operational Land Imager) sensor, orbit/point 219/062. We used LaSRC data (*Landsat 8 Surface Reflectance Code*, Vermote et al. 2016) from the Collection-1 that are radiometrically calibrated and orthorectified using ground points and digital elevation model data to correct for relief displacement, and also the on-demand Level-2 products that corrects the images for atmospheric effects at surface reflectance level (USGS 2018). All images were ordered and downloaded from the USGS (U. S. Geological Survey web page).

The images were collected from June 21st, 2016, November 12th, 2016 and November 28th, 2016. The

characteristics regarding the image collection geometry are: image of June 21st, 2016 (cloud cover: 5.7%; solar elevation angle: 52.20°; azimuthal angle: 44.36°); image of November 12th, 2016 (cloud cover: 9.12%; solar elevation angle: 62.68°; azimuthal angle: 124.91°); image of November 28th, 2016 (cloud cover: 9.35%; solar elevation angle: 59.98°; azimuthal angle: 130.08°). The choice of the images on the dates mentioned above was related to the similarity of their climatic conditions with the period of field data collection. Although the image dates are approximately six months, one month before and one year after, respectively, the start of field data collection, it was assumed that the variation of amount vegetation biomass values in the region was not significant during this period.

Initially six bands were used and eight spectral indexes were calculated: RVI (Pearson and Miller, 1972); NDVI (Rouse et al. 1974); SAVI (Huete, 1988); EVI (Huete et al. 1997); NDWI (Gao, 1996); GNDVI (Gitelson et al. 1996); MNDWI (Xu 2006); and CTVI (Perry and Lautenschlager 1984). These indices were chosen because they are directly related to vegetation (RVI, NDVI, GNDVI, EVI and CTVI), soil (SAVI) and water (NDWI and MNDWI).

The first investigation was to adjust equations to better understand the relationship between biomass and remote sensing variables. Therefore, an exploratory data analysis was performed by means of data frequency distribution and the correlation between vegetation biomass as a dependent variable and remote sensing variables as independent variables.

The equations were adjusted considering biomass as the dependent variable and all vegetation bands and indexes as the independent variables, seeking the adjustment with the smallest possible number of independent variables. The *stepwise backward* selection method was used to select the most significant independent variables. This method initially fits a model with all variables and then eliminates one by one (Silva 2016). Of the fourteen independent variables evaluated in all scenes (six bands and eight indexes), only one variable for the image of June 21st, 2016, three variables for the image of November 12th, 2016 and two variables for the image of November 28th, 2016 were significant.

In the next step, we applied multiple linear regression analysis, in which was considered as significant independent variables selected by the algorithm to construct the prediction model.

Validation measures, such as the coefficient of determination (R^2), the mean absolute error (MAE) and the root mean square error (RMSE) were calculated in order to evaluate the performance of the estimates for each evaluated date. Estimates were used for AGB spatialization at all dates for the study area. The statistical steps were performed in the R statistical software (R Core Team 2017).

Results

For total vegetation biomass and biomass carbon stock, the analysis of variance indicated significant differences between the vegetation ($p < 0.01$). Through the Tukey test, it was observed that the mangrove evergreen vegetation presented the highest averages for vegetation biomass (517.43 Mg ha^{-1}) and plant carbon stock (258.34 Mg ha^{-1}), for the significant difference of $p < 0.01$. The psammophile pioneer vegetation presented the smallest amount ($p < 0.05$). There was also a similarity between the variables of floodplain, carnaubals and dune subevergreen vegetations (Fig. 5).

The floodplain, carnaubals and dune subevergreen vegetations obtained statistically similar amounts of biomass. The same behavior was presented for carbon stock results. For the psammophile pioneer vegetation, the vegetation biomass ranged from 6.68 to 12.92 Mg ha^{-1}, presenting the lowest average biomass per hectare (9.22 Mg ha^{-1}) in the study area.

It was observed that 57.62% of MEV (mangrove evergreen vegetation) presented DBH above 30 cm. Regarding height, it was observed that 52.54% of the individuals presented heights higher than 20 m. The FV (floodplain vegetation) presented 48.5% of the individuals; and the VC (vegetation associated with carnaubals) presented 29.3% of the individuals in this condition of DBH. Regarding DSV (dune subevergreen vegetation), there was a large number of individuals with DBH below 30 cm (89.13% of the total).

The description of remote sensing AGB prediction models is presented in Table 1. In the estimate, the highest values for R^2 and R^2aj and the lowest values for SQR were observed for the image models of June 21st and November 12th, 2016. However, the lowest

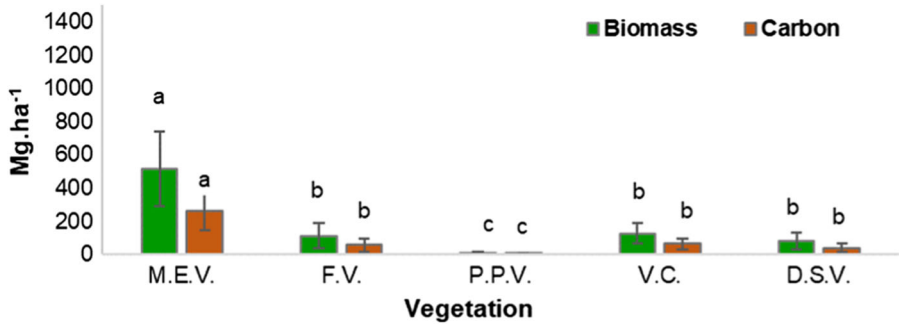

Fig. 5 Mean biomass and carbon from biomass in different types of vegetation in PRD. MEV (mangrove evergreen vegetation), FV (floodplain vegetation), PPV (pioneer psamophilic vegetation), VC (carnaubal vegetation) e DSV (dune subpereniferous vegetation). Means followed by same letter do not differ by Tukey test. CVbiomass: 38.24%; CVcarbon: 35.84%

Table 1 Description of the models obtained by treatment

Dates	Model						
	Explanatory Variables	NV	R^2	R^2_{aj}	SQR	MAE	RMSE (Mg ha^{-1})
June 21th, 2016	MNDWI***	1	0.61	0.60	239,482.00	− 109.994	276.04
	BIO = 212.62 + 680.31 MNDWI						
November 12th, 2016	Banda 7***, EVI**, MNDWI***	3	0.74	0.72	158,199.00	6.84	47.89
	BIO = 825.99 − 0.0973Banda7 − 225.82 EVI + 1164.55 MNDWI						
November	Banda 7**, MNDWI***	2	0.60	0.58	245,521.00	9.63	34.67
28th, 2016	BIO = 260.369 − 0.01671Banda 7 + 529.617 MNDWI						

Where: *NV* is the number of variables selected by *stepwise backward*, including the constant, R^2 is the coefficient of determination, R^2aj is the adjusted coefficient of determination, *SQR* is the sum of the squares of the residuals, *MAE* is the mean absolute error, *RMSE* is the square root of the mean square error

*$p < 0.05$; **$p < 0.01$; ***$p < 0.001$

Table 2 Prediction statistical errors calculated for each vegetation type of the PRD, for the images of June 21th, 2016, November 12th, 2016 and November 28th, 2016, where: MAE (mean absolute error); RMSE (square root of mean square error); MEV (mangrove evergreen vegetation), FV (floodplain vegetation), PPV (pioneer psamophilic vegetation), CV (carnaubal vegetation) and DSV (dune subpereniferous vegetation)

Vegetation	June 21th, 2016		November 12th, 2016		November 28th, 2016	
	MAE	RMSE	MAE	RMSE	MAE	RMSE
M.E.V	87.66	146.59	56.65	157.49	98.28	92.20
F.V	− 78.96	87.90	− 49.36	112.10	− 104.84	62.40
V.C	65.56	97.31	37.82	98.80	59.45	73.59
D.S.V	− 3.98	60.56	1.34	51.93	− 25.40	67.32
P.P.V	− 67.66	80.17	12.52	36.39	− 2.57	30.72

values for MAE and RMSE were observed in the models obtained from the images of November 12th, 2016 and November 28th, 2016, being considered the best models to estimate AGB. The predicted errors MAE and RMSE calculated for each vegetation on each image date are presented in Table 2. Given the

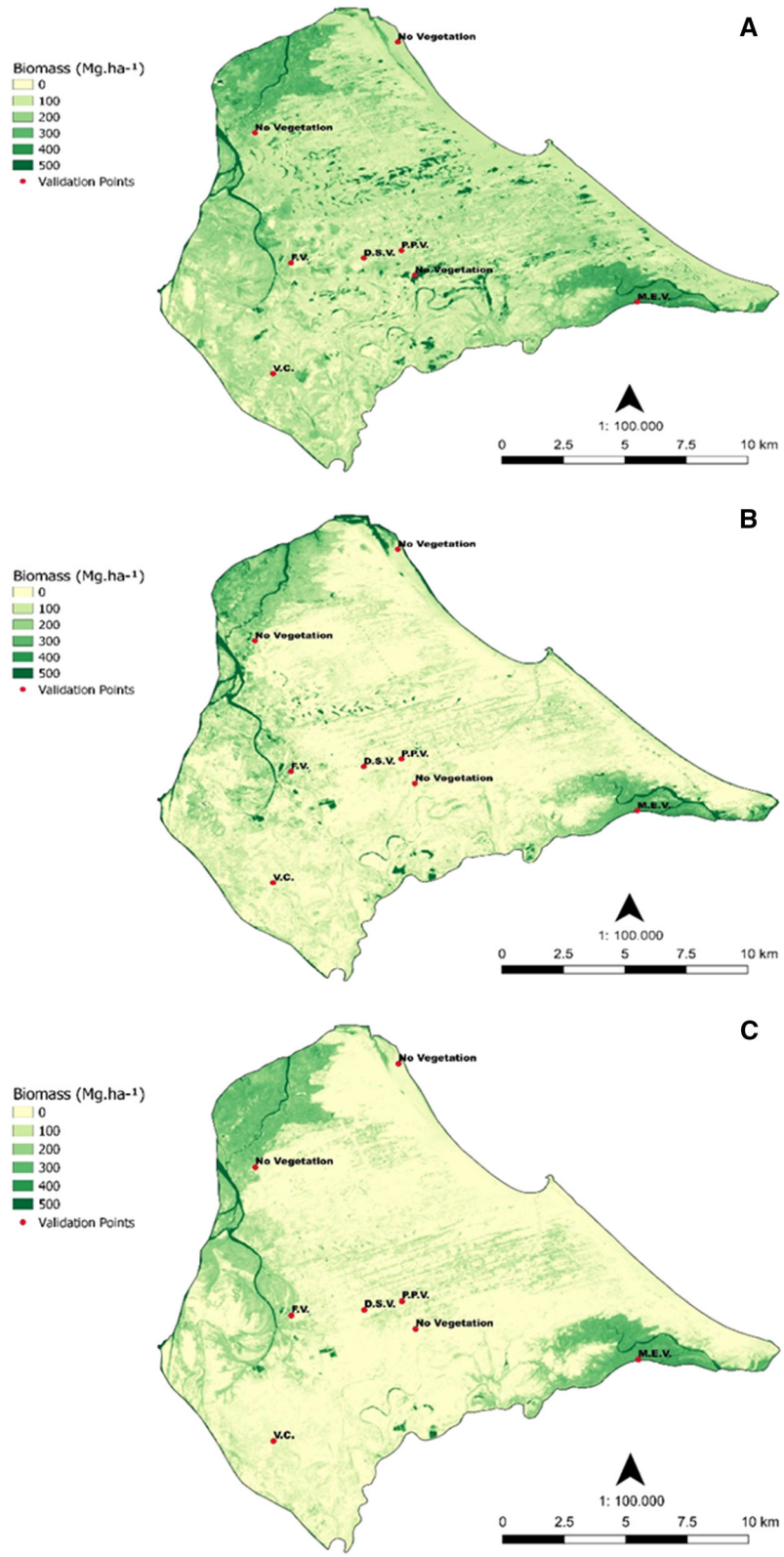

Fig. 6 Estimated above ground biomass (Mg ha^{-1}) of the PRV vegetation based on models using data from Landsat-8 OLI: **a** on June 21th, 2016 (MNDWI); **b** November 12th, 2016 (band 7, EVI, MNDWI); and **c** November 28th, 2016 (band 7, MNDWI). Where: MEV (mangrove evergreen vegetation), FV (floodplain vegetation), PPV (pioneer psamophilic vegetation), CV (carnaubal vegetation) and DSV (dune subpereniferous vegetation)

results, we obtained the spatial distribution of AGB for the dates with the best results (Fig. 6).

Discussion

Biomass Calculated by Allometric Equations

In the case of mangrove evergreen vegetation, several morphological and physiological characteristics are responsible for making this vegetation a great biomass producer and carbon sequestered, when compared to the other studied vegetation. Naidoo (2016) points out that mangroves grow on soft substrates, endowed with organic matter, which contribute to these plants growing and having high biomass contents and, consequently, high carbon stocks.

The flood condition develops adaptations, which include modifications in the walls of plant tissues, in the shape and size of the roots of the mangrove species, and in the photosynthetic rates that directly influence the resistance of these species, especially under conditions of high salinity, as is the case of the studied environment.

Although salinity is a limiting condition for some mangrove species, where the higher the salinity, the lower the growth rates and carbon gains (Nguyen et al. 2015), it was found the presence of species more resistant to these conditions, indicating the adaptation to the presented conditions. This scenario was perceived due to the large size of the individuals and the presence of a single species, with individuals with similar dendrometric characteristics, in all evaluated plots, which results in higher biomass contents than in forests with diversity of mangrove species.

Research conducted in the world over the past six years (Hickey et al. 2018; Kamruzzaman et al. 2017; Tang et al. 2016; Wang et al. 2013; Ray et al. 2013) showed variations in average values of biomass. In Brazil, in mangroves of the Amazon region, for example Kauffman et al. (2018), reported vegetation biomass lower than average observed in this study using the same allometric equations Fonseca and Mochel (2016). estimated the mangrove biomass of three species in São Luís, Maranhão and observed average value of total biomass for *R. mangle* species, lower than that observed in this study, using an allometric equation developed by the authors (Table 3).

The biomass observed in mangroves in Japan, West Africa and India, as well as the biomass observed in mangroves in Brazil mentioned above, were lower than those reported in this study, even using the same equations as the authors and considering the measured dendrometric characteristics, which differ mainly. the climatic conditions of these places and the geographical position, as indicated by Saintilan et al. (2014). However, even with similar dendrometric characteristics, such as height, mangrove forests can have different increments of AGB. The density of plant individuals in the plots highlights the influence of this factor in the calculation of AGB and highlights the need to develop regional allometric equations (Simard et al. 2018).

As for the height, in some mangroves evaluated, it was possible to measure individuals with height higher than 40 m, a factor that, combined with the thick DBH of many individuals, directly influence the results obtained from the equations used.

Fonseca and Mochel (2016) observed in mangroves from the Brazilian estate of Maranhão individuals of *R. mangle* with average DBH of 13.1 cm and average height of 15 m and consider these parameters as determining factors in the total vegetation biomass of a forest fragment, as these are the holders of the highest biomass content in the plant. A second important factor is the use of allometric equations, which in the case of the study, were specific to the northeast region of Brazil, especially when it comes to *R. mangle* species, unlike the studies mentioned above, which despite using equations that consider the same parameters considered in this work, they used equations developed for mangroves in tropical regions globally.

Simard et al. (2018), analyzing the distribution of mangrove height in Africa, observed a relationship of higher productivity in terms of AGB to the higher forests. The authors also relate that this increase is related to mangroves present in estuarine areas, which are more cloudy and humid. Another characteristic highlighted by the authors is that regions with mangroves of greater height and greater AGB, are associated with environments dominated by rivers and with low housing density. This condition coincides with the characteristics of some mangrove areas evaluated, especially those in which the individuals had the highest heights.

Table 3 Mean values of biomass using allometric equations developed in the literature

Location (Authors)	Equation	Average value biomass observed by the authors	Average value biomass observed in this study*
Australia (Hickey et al. 2018)	Saenger and Snedaker (1993)	70 Mg ha^{-1}	220.02 Mg ha^{-1}
Japan (Kamruzzaman et al. 2017)	Comely and McGuinnes (2005)	162.7 Mg ha^{-1}	208.62 Mg ha^{-1}
Atlantic coast of west Africa (Tang et al. 2016)	Saenger and Snedaker (1993)	196.17 Mg ha^{-1}	220.02 Mg ha^{-1}
Southern China (Wang et al. 2013)	Comley and McGuinnes (2005)	270.59 Mg ha^{-1}	208.62 Mg ha^{-1}
India (Ray et al. 2013)	Ray et al. (2011)	37.78 Mg ha^{-1}	180.54 Mg ha^{-1}
Amazon region (Kauffman et al.2018)	Fromard et al. (1998)	290 Mg ha^{-1}	343.52 Mg ha^{-1}
São Luís, NE Brazil (Fonseca and Mochel 2016)	Own authors	50.49 Mg ha^{-1}	284.06 Mg ha^{-1}

*Values calculated with the same equations used by the authors cited

When establishing a comparison with the primary Amazon forest Lu et al. (2005), observed AGB values between 110 and 490 Mg ha^{-1} with an average of 248 Mg ha^{-1}. Chambers et al. (2001) found values etween 232 and 391 Mg ha^{-1} for the central Amazon. The results indicate the great potential of carbon stock in the mangroves of the Piauí coast.

Regarding the vegetation carbon stock, considering the conversion factor proposed by the Intergovernmental Panel on Climate Change (IPCC), which indicates that the amount of carbon stored in the vegetation biomass is around 50% (IPCC 2007), the estimated values for this variable are derived from the relationship between the biomass obtained by the allometric equations and the conversion factor. Therefore, this result is directly related to the vegetation biomass data.

Pinto et al. (2016), calculating the carbon absorption in a mangrove forest in the Brazilian state of São Paulo, observed that the studied species had capacity to store 0.08 Mg ha^{-1} of carbon. Sitoe, Mandlate and Guedes (2014) observed that the mangrove forests in Mozambique store around 58.60 Mg ha^{-1} of carbon, values below those observed in this work. The mentioned authors highlight the relationship between biomass carbon stock and tree height, being a directly proportional relationship.

In contrast, in the tropical Pacific regions, Kauffman and Donato (2012) observed the carbon storage of mangrove vegetation biomass ranging from 169 to 452 Mg ha^{-1}. Kauffman and Bhomia (2017) observed carbon reservoirs in Central West African mangroves ranging from 5.2 to 312 Mg ha^{-1}. Similarly, Kauffman et al. (2018) reported carbon stocks in Amazon mangroves approaching 145 Mg ha^{-1}.

Compared to the global average carbon stock in mangroves above ground, which is 82 Mg C ha^{-1} (IPCC 2014), the average above-ground carbon stock observed in the mangroves of the PRD is higher than the default value (190.44 Mg C ha^{-1}) proposed.

The observed behavior for biomass of FV, VC and DSV can be explained by the physiological behavior of plants. Although they are in different soil types, number of individuals and species, they are present in areas that may be flooded in the rainy season and subsequently subject to water stress in the driest months.

This condition leads to the development of morphoanatomic adaptations, especially in palm trees such as *M. flexuosa*, *E. oleracea* and *C. prunifera*, to support soil oxygen reduction. Thus, these species can maintain their high photosynthetic rate even under flooding, continuing their biomass production regardless of the period of the year (Arruda and Calbo 2004), reaching biomass similar to those of large trees such as *A. occidentale,* found in the dune subevergreen vegetation.

Analyzing the average of the vegetation biomass values reported by the dune subevergreen vegetation (78.30 Mg ha^{-1}), it was found higher biomass in relation to that reported by Santos et al. (2016), who observed the biomass, in vegetation with Caatinga species in NE, Brazil, of 12 Mg ha^{-1}. Considering the use of allometric equations of Lima Junior et al. (2014), to calculate the biomass in the dune subevergreen vegetation, was also observed higher values than those reported by the authors, which ranged from 5.93 to 60.74 Mg ha^{-1}.

Although DBH has a direct influence on biomass, the small percentage of individuals with DBH above 30 cm in DSV. may have increased the biomass content of this vegetation. In addition, height, being considered a determining factor for biomass, also directly influenced the result, given that 44.6% of the individuals presented height above 12 m, with plants up to 20 m high.

In this context, Sausen et al. (2013) highlight that, in native forests, the occurrence of certain large species is the main factor promoting increase in biomass and carbon stocks. In addition, the authors point out that some species contribute more intensely to carbon stocks, and the increase in stocks is directly proportional to the volume of wood. Simply put, the higher the wood density, the higher the biomass stocked per cubic meter of wood (Carneiro et al. 2014).

As for the psammophile pioneer vegetation, the results for biomass are directly related to the size of the analyzed vegetation, which is composed of creeping plants, tolerant to high substrate mobility, which occur in places with low organic matter availability, rapid water drainage, direct and intense sunlight causing overheating during some hours of the day, especially in the warmer months (Andrade, 1966).

Given the conditions mentioned above, these plants are underdeveloped, and consequently have low amounts of biomass, even covering large ranges, which justifies the lower values for biomass recorded in this study and consequently low carbon stock averages (4.61 Mg ha^{-1}).

Fidelis et al. (2012) evaluated wetlands in the Brazilian Cerrado and observed biomasses that reached up to 15.92 Mg ha^{-1}, which is not far from the highest biomass value recorded for psammophile pioneer vegetation. In contrast, Rocha and Miranda (2012) quantified the biomass of the savanna environment tree stratum in the Amazon and observed biomass values that did not exceed 2.5 Mg ha^{-1}, lower than that observed in the psammophile pioneer vegetation.

Although when compared to the other vegetation studied, the biomass of the psammophile pioneer vegetation is low, the average observed was also higher than those attributed by Bokhorst et al. (2017) for bush and grass vegetation in the Falkland Islands of 2.77 Mg ha^{-1}. The authors associated the result with the intense use of herding in the region. Results with lower values were also reported by Chabi et al. (2015), who observed biomass in herbaceous savanna areas in Sudan, ranging from 0.06 to 9.2 Mg ha^{-1}.

Regression models for estimated biomass

Highlighting the exploratory analysis of the image data on June 21 st, 2016, we found a strong positive correlation between biomass and MNDWI. For the image of November 12th, 2016, it was observed that EVI and band 7 (OLI, Landsat-8) showed a moderate correlation with the predicted biomass. However, the changes in biomass relative to changes in band 7 occur inversely, observed by the trend line indicating a decrease in vegetation biomass with increasing reflectance values in band 7. A similar result was observed by Wu et al. (2016), who estimated the vegetation biomass of a forest in northeastern China and reported a correlation of biomass with band 7 of -0.566.

The MNDWI showed a strong positive correlation with the predicted biomass, so that the vegetation biomass presents growth in approximately the same proportion of the independent variable. Exploratory analysis of the predicted image model of November 12th, 2016 indicated that AGB showed a strong positive correlation with MNDWI. On the other hand, it presented a moderate and negative correlation with the band 7.

Risdiyanto and Fakhrul (2017) reported that high above-ground biomass values in Indonesian forests were about 63.06% related to the low reflectance values in band 7 of Landsat-8 OLI sensor. The same authors indicate that variations in the estimated canopy biomass occur mainly due to the heterogeneity of the vegetation and the influence of humidity, characteristics similar to the vegetation of the present study.

In all models generated for the scenes, it was observed that the MNDWI was present as an explanatory variable, presenting greater sensitivity in the detection of AGB in the study area. This result is related to the conditions of the study site, characterized by being a region in contact with water, influenced by tidal movement, presenting some flooded areas. In addition, the MNDWI is an index that improves the efficiency of identification of water bodies and the reduction of noise produced by areas with vegetation or exposed soil, as well as some species have a higher concentration of water in the leaves and, consequently, indexes like MNDWI tend to give better results.

Barrachina et al. (2015), estimating biomass in the Pyrenees prairie vegetation in southwestern Europe, also observed that MNDWI showed a strong relationship with vegetation biomass. According to the authors, although spectral indexes such as NDVI, EVI, and GNDVI are a priori more related to biomass production, those related to moisture play an important role in the modeling of AGB, especially in regions influenced by water bodies, being statistically more selected than other indexes, which occurred in the three models of AGB estimates, developed for the area of the Parnaiba river Delta. Thus, the medium infrared ranges are crucial descriptors in the estimation of AGB in the area studied in this work.

Unlike other studies, NDVI was not considered as an explanatory variable in the developed models, not influencing the estimates. Nakai (2016) also observed a low correlation between NDVI and biomass, being less sensitive in estimating this dependent variable in relation to EVI, similarly to that observed in the present study. According to the author, EVI is more sensitive to leaf fall and responds better to canopy stratification and architecture characteristics, being more sensitive for dense vegetation detection.

Alba et al. (2017) also observed the absence of significant correlation between NDVI and biomass in 18-year-old *Eucalyptus grandis* canopies and related this result to the fact that the vegetation presents dissimilarity in tree height within the sample units, influencing the same shading points in flat areas and reducing the reflectance of electromagnetic radiation in the near infrared spectral range.

It should be noted that although the spectral bands and some indexes that are directly related to the canopy structure are more sensitive and statistically more significant than others, the biomass estimation models incorporated the humid condition of the study area. This statement can be verified in the presence of MNDWI in all prediction models elaborated in this study and band 7 in at least two models Barsi et al. (2014) indicate that the use of band 7 in mappings helps to identify the best water content in vegetation, which was probably identified in this work.

The prediction statistical errors for each vegetation on each image date indicate that the biomass values estimated by multiple linear regression models showed discrepant behaviors. MEV was the one that presented the most errors in AGB estimates. When compared with the other vegetation studied, the mean absolute error indicated that there was overestimation of values in the estimate. It was also observed that the variables used in the image of November 28th, 2016 obtained the lowest RMSE.

Overall, the maps indicate that the highest biomass values are concentrated in lowland areas with MEV and the intermediate values in areas corresponding to terraces and plains under FV and some areas under VC. These areas presented AGB of 150 Mg ha^{-1}. The lowest values were observed in areas corresponding to DSV and PPV. These areas presented biomass below 50 Mg ha^{-1}.

The results presented by the RMSE of the two spatializations are confirmed when the validation points used for each studied vegetation are compared. The estimated AGB for these points indicates that the points corresponding to MEV, despite having the highest RMSE, nevertheless recorded higher AGB when compared to other vegetation, followed by FV and VC. It is also noteworthy that the geometry of data acquisition interfered with the lighting geometry of the scenes, where the image with the lowest solar elevation angle (image of June 21 st, 2016) suffers the decrease of solar irradiance on the surface due to greater shading, especially in transition areas between one vegetation and another. These effects are manifested in surface reflectance variations and consequently in vegetation indexes values and in model-derived biomass estimates.

These vegetations, although having different amounts of biomass, in general, represent important carbon stockpiles. The highest values of plant biomass are mainly associated with the structure of vegetation, the density and conservation of forests. Similar to the maps developed by Simard et al. (2018), although only

for mangrove forests, the models developed in this work resulted in maps that represent vegetation as a major carbon store and show considerable spatial distribution.

Although the region is an area of sustainable use and with the presence of housing, agricultural activities and tourism, this condition has had a positive influence on the quantification of biomass, given that the rational use of natural resources contributes to the conservation of species.

Pavani et al. (2018), point out that the limitations imposed on areas of environmental protection guarantee the conservation of vegetation that holds an offer of ecosystem services. This situation implies higher values of plant biomass, when compared to the vegetations most impacted by anthropic actions and, consequently, greater carbon stocks.

The authors report that areas of coastal vegetation impacted by man may release, in future scenarios, up to 4 million Mg ha^{-1} of carbon into the atmosphere. These losses can reduce the benefits generated by the ecosystem, such as climate regulation and can intensify the negative impacts of climate change.

Conclusions

There is a great variability of vegetation biomass in the PRD according to the different types of vegetation and landscape present. The mangrove evergreen vegetation has a higher amount of vegetation biomass and, consequently, a greater storage potential than other vegetation in the PRD.

Psammophile pioneer vegetation has the lowest amount of vegetation biomass and, consequently, the lowest carbon storage potential. The lighting geometry of the scenes and the time of year resulted in different behaviors in the estimation of vegetation biomass.

The combination of biomass data calculated by allometric equations and sensing data is possible to be performed with significant precision for the PRD vegetation, indicating that the work can be extended to other coastal environments.

The condition of a conservation area for sustainable use contributes to this region being a large stocking of carbon from plant biomass. Although studies on biomass and plant carbon estimates are highly complex, especially in mangrove areas, this study, in particular, is a starting point for future and more comprehensive research for coastal areas in northeastern Brazil.

Acknowledgements The authors especially thank the Conselho Nacional de Desenvolvimento Científico e Tecnológico – CNPq for Scholarship PQ2 (301254/2017-6; G.S. Valladares), and the Coordenação de Aperfeiçoamento de Pessoal de Nível Superior - CAPES for Scholarship (M.G.T. Portela).

References

Alba E et al (2017) Uso de imagens de média resolução espacial para o monitoramento de dosséis de Eucalyptus grandis. Sci Agraria 18:1–8. https://doi.org/10.5380/rsa.v18i4.51944

Alongi DM (2014) Carbon cycling and storage in mangrove forests. Ann Rev Mar Sci 6(1):195–219

Barsi JA et al (2014) The spectral response of the landsat-8 operational land imager. Remote Sens 6:10232–10251. https://doi.org/10.3390/rs61010232

Barrachina M, Cristóbal H, Tulla AF (2015) Estimating above-ground biomass on mountain meadows and pastures through remote sensing. Int J Appl Earth Obs Geoinf 38:184–192. https://doi.org/10.1016/j.jag.2014.12.002

Bokhorst S et al (2017) Dwarf shrub and grass vegetation resistant to long-term experimental warming while microarthropod abundance declines on the Falkland Islands. Aust Ecol 42:984–994. https://doi.org/10.1111/aec.12527

Brazil (1996) Decreto de 28 de Agosto de 1996. Dispõe sobre a criação da Área de Proteção Ambiental Delta do Parnaíba, nos Estados do Piauí, Maranhão, e Ceará, e dá outras providências, 1996.

Brazil (2000) Lei n° 9.985, de 18 de julho de 2000. Regulamenta o art.225, §1°, incisos I, II, III e IV da Constituição Federal, institui o Sistema Nacional de Unidades de Conservação da Natureza e dá outras providências

Brazil (2000b) Decreto de 16 de novembro de 2000. Cria a Reserva Extrativista Marinha do Delta do Parnaíba, no Município de Ilha Grande de Santa Isabel, Estado do Piauí, e nos Municípios de Araióses e Água Doce, Estado do Maranhão, e dá outras providências. Disponível em: https://www.planalto.gov.br/ccivil_03/DNN/DNN9084.htm , acesso em 28 de março de 2019

Brown S, Gillespie AJR, Lugo AEL (1989) Biomass estimation methods for tropical forests with applications to forest inventory data. For Sci 35:881–902. https://doi.org/10.1093/forestscience/35.4.881

Cabral LJRS (2018) Levantamento pedológico da planície do Delta do Parnaíba, PI. Dissertação (Mestrado em Geografia), Centro de ciências Humanas e Letras, Universidade Federal do Piauí, Teresina, 2018

Carneiro ACO et al (2014) Potencial energético da madeira de Eucalyptus sp. em função da idade e de diferentes materiais genéticos. Rev Árvore 38:375–381. https://doi.org/10.1590/S0100-67622014000200019

Chambers JQ et al (2001) Tree damage, allometric relationships, and above-ground net primary production in central Amazon forest. For Ecol Manag 152:73–84

Comley BWT, Mcguinness KA (2005) Above- and below-ground biomass, and allometry, of four common northern Australian mangroves. Aust J Bot 53:431–436

Cusack M et al (2018) Organic carbon sequestration and storage in vegetated coastal habitats along the western coast of the Arabian Gulf. Environ Res Lett 13(7):074007

de Paula Filho FJ, Marins RV, Lacerda LD de (2015) Natural and anthropogenic emissions of N and P to the Parnaíba River Delta in NE Brazil. Estuar Coast Shelf Sci 166:34–44

Duncan C et al (2018) Satellite remote sensing to monitor mangrove forest resilience and resistance to sea level rise. Methods Ecol Evol 9:1837–1852. https://doi.org/10.1111/2041-210X.12923

Fatoyinbo T et al (2018) Estimating mangrove aboveground biomass from airborne LiDAR data: a case study from the Zambezi River delta. Environ Res Lett 13(2):025012

Fidelis A, Lyra MFS, Pivello VR (2012) Above- and below-ground biomass and carbondynamics in Brazilian Cerrado wet grasslands. J Veg Sci 24:356–364. https://doi.org/10.1111/j.1654-1103.2012.01465

Fonseca ILA, Mochel FR (2016) Fitomassa aérea de um manguezal no estuário do rio dos cachorros, São Luís, Maranhão, Brasil. Boletim Lab Hidrobiol 26:17–25

Frangi JL, Lugo AE (1985) Ecosystem dynamics of a subtropical floodplain forest. Ecolog Monogr 55:351–369. https://doi.org/10.2307/1942582

Fromard F et al (1998) Structure, above-ground biomass and dynamics of mangrove ecosystems: new data from French Guiana. Oecologia 115:39–53. https://doi.org/10.1007/s004420050

Fernandes AG et al (1996) IV-Componentes biológicos: Vegetação. CEPRO, Macrozoneamento Costeiro do Estado do Piauí: relatório geo-ambiental e sócio-econômico. Teresina, Fundação CEPRO, pp 43–72

Frank D et al (2015) Effects of climate extremes on the terrestrial carbon cycle: concepts, processes and potential future impacts. Glob Chang Biol 21(8):2861–2880

Fundacion Solar (2010) Elementos técnicos para inventários de carbono em uso del solo. Guatemala

Gao B (1996) A normalized difference water index for remote sensing of vegetation liquid water from space. Remote Sens Environ 58:257–266. https://doi.org/10.1016/S0034-4257(96)00067-3

Gitelson AA, Kaufman YJ, Merzlyak MN (1996) Use of a green channel in remote sensing of global vegetation from EOS-MODIS. Remote Sens Environ 58:289–298. https://doi.org/10.1016/S0034-4257(96)00072-7

Guzzi A (2012) Biodiversidade do Delta do Parnaíba: litoral piauiense. EDUFPI, Parnaíba

Hickey SM et al (2018) Spatial complexities in aboveground carbon stocks of a semi-arid mangrove community: a remote sensing height-biomass-carbon approach. Estuar Coast Shelf Sci 200:194–201. https://doi.org/10.1016/j.ecss.2017.11.004

Huete AR (1988) A soil adjusted vegetation index (SAVI). Remote Sens Environ 25:295–309. https://doi.org/10.1016/0034-4257(88)90106-X

Huete AR et al (1997) A comparison of vegetation indices over a global set of TM images for EOS-MODIS. Remote Sens Environ 59:440–451. https://doi.org/10.1016/S0034-4257(96)00112-5

Intergovernmental Panel on Climate Change (IPCC) (2007) Climate change 2007: the scientific basis summary for policymakers. Contribution of Working Group I to the Fourth Assessment Report of the Intergovernmental Panel on Climate Change. Cambridge University Press, Cambridge

Intergovernmental Panel on Climate Change (IPCC) (2014) Supplement to the 2006 IPCC Guidelines for National Greenhouse Gas Inventories. In: Wetlands, Hiraishi T, Krug T, Tanabe K, Srivastava N, Baasansuren J, Fukuda M, Troxler TG (eds) IPCC, Switzerland

Kamruzzaman Md et al (2017) Species composition, biomass, and net primary productivity of mangrove forest in Okukubi River, Okinawa Island, Japan. Reg Stud Mar Sci 12:19–27

Kauffman JB, Donato DC (2012) Protocols for the measurement, monitoring, and reporting of structure, biomass and carbon stocks in mangrove forests. CIFOR Working Paper 86. Center for International Forest Research, Indonesia

Kauffman JB, Bhomia RK (2017) Ecosystem carbon stocks of mangroves across broad environmental gradients in West-Central Africa: global and regional comparisons. PLoS ONE 7(12):1–17. https://doi.org/10.1371/journal.pone.0187749

Kauffman JB et al (2018) Carbon stocks of mangroves and salt marshes of the Amazon region. Brazil Biol Lett 14:1–4. https://doi.org/10.1098/rsbl.2018.0208

Komiyama A, Poungparn S, Kato S (2005) Common allometric equations for estimating the tree weight of mangroves. J Trop Ecol 21:471–477. https://doi.org/10.1017/S0266467405002476

Lima Júnior C et al (2014) Estimation of "caatinga" woody biomass using allometric equations and vegetation index. For Sci 42:289–298

Lu D, Batistella M, Moran E (2005) Satellite estimation of aboveground biomass and impacts of forest stand structure. Photogr Eng Remote Sens 71:967–974

Macdicken K (1997) A guide to monitoring carbon storage in forestry and agroforestry projects. Institute for Agricultural Development, Winrock International, Arlington

Maia GN (2004) Caatinga: árvores e arbustos e suas utilidades. Leitura & Arte, São Paulo

Naidoo G (2016) The mangroves of South Africa: an ecophysiological review. S Afr J Bot 107:101–113. https://doi.org/10.1016/j.sajb.2016.04.014

Nakai ES (2016) Quantificação da biomassa e estoque de carbono em diferentes coberturas vegetais por meio de sensoriamento remoto. Piracicaba, Escola Superior de Agricultura "Luiz de Queiroz", Tese (Doutorado em Ciências)

Naessens W, Maere T, Nopens I (2012) Critical review of membrane bioreactor models. Part 1: Biokinetic and filtration models. Biores Technol 122:95–106. https://doi.org/10.1016/j.biortech.2012.05.070

Neubauer SC, Megonigal JP (2019) Correction to: moving beyond global warming potentials to quantify the climatic role of ecosystems. Ecosystems 22(8):1931–1932

Nguyen HT et al (2015) Growth responses of the mangrove Avicennia marina to salinity: development and function of shoot hydraulic systems require saline conditions. Ann Bot. https://doi.org/10.1093/aob/mcu257

Pavani BF et al (2018) Estimating and valuing the carbon release in scenarios of land-use and climate changes in a Brazilian coastal area. J Environ Manag 226:416–427. https://doi.org/10.1016/j.jenvman.2018.08.059

Pearson RL, Miller LD (1972) Remote mapping of standing crop biomass for estimation of the productivity of short-grass prairie, Pawnee National Grasslands, Colorado. In: Proceedings of the 8th international symposium on remote sensing of the environment, Ann Arbor, MI, 2, 1355–1379

Perry CR, Lautenschlager LF (1984) Functional equivalence of spectral vegetation indices. Remote Sens Environ 14:169–182. https://doi.org/10.1016/0034-4257(84)90013-0

Pinto LM et al (2016) Sequestro de carbono atmosférico no bosque do manguezal da APA da Serra do Guararú, Guarujá-SP. UNISANTA Biosci 5:51–57

Ray R et al (2013) Improved model calculation of atmospheric CO_2 increment in affecting carbon stock of tropical mangrove forest. Tellus 65:1–11. https://doi.org/10.3402/tellusb.v65i0.18981

Ray R et al (2011) Carbon sequestration and annual increase of carbon stock in a mangrove forest. Atmos Environ 45:5016–5024. https://doi.org/10.1016/j.atmosenv.2011.04.074

R Core Team (2017) R: a language and environment for statistical computing. Vienna, Austria: R Foundation for Statistical Computing. Disponível em: https://www.R-project.org/

Risdiyanto I, Fakhrul M (2017) Examination of multi-spectral radiance of the Landsat 8 satellite data for estimating biomass carbon stock at wetland ecosystem. Preprints 1:1–14. https://doi.org/10.20944/preprints201704.0020

Rocha AES, Miranda IS (2012) Cobertura vegetal, biomassa aérea e teor de proteína do estrato herbáceo de ambiente savânico no município de Maracanã, Pará, Brasil. Rev Bras Biociênc 10:513–520

Rouse JW et al (1974) Monitoring the vernal advancement of retrogradation (greenwave effect) of natural vegetation. NASA/GSFC, Type III, Final Report, Greenbelt, MD

Saintilan N et al (2014) Mangrove expansion and salt marsh decline at mangrove poleward limits. Glob Change Biol 20:147–157. https://doi.org/10.1111/gcb.12341

Saenger P, Snedaker SC (1993) Pantropical trends in mangrove above-ground biomass and annual litterfall. Oecologia 96:293–299

Santos HVS et al (2017) Allometric models for estimating the aboveground biomass of the mangrove *Rhizophora mangle*. Bras J Oceanogr 65:44–53

Santos RC et al (2016) Estoques de volume, biomassa e carbono na madeira de espécies da Caatinga em Caicó, RN. Pesqui Florest Bras 36:1–7. https://doi.org/10.1590/s1679-87592017127006501

Silva AGA da et al (2019) Coastline change and offshore suspended sediment dynamics in a naturally developing delta (Parnaíba Delta, NE Brazil). Mar Geol 410:1–15

Simard M et al (2018) Mangrove canopy height globally related to precipitation, temperature and cyclone frequency. Nat Geosci 12(1):40–45. https://doi.org/10.1038/s41561-018-0279-1

Tang W et al (2016) The assessment of mangrove biomass and carbon in West Africa: a spatially explicit analytical framework. Wetlands Ecol Manag 24:153–171. https://doi.org/10.1007/s11273-015-9474-7

Vermote E et al (2016) Preliminary analysis of the performance of the landsat 8/oli land surface reflectance product. Remote Sens Environ 185:46–56. https://doi.org/10.1016/j.rse.2016.04.008

Wang G et al (2013) Ecosystem carbon stocks of mangrove forest in Yingluo Bay, Guangdong Province of South China. For Ecol Manag 310:539–546. https://doi.org/10.1016/j.foreco.2013.08.045

Xu H (2006) Modification of normalised difference water index (NDWI) to enhance open water features in remotely sensed imagery. Int J Remote Sens 27:3025–3033. https://doi.org/10.1080/01431160600589179

Zhang C et al (2018) Quantification of sawgrass marsh aboveground biomass in the coastal Everglades using object-based ensemble analysis and Landsat data. Remote Sens Environ 204:366–379